

PVP2018-84898

GLOBAL HARMONIZATION OF FATIGUE LIFE TESTING IN GASEOUS HYDROGEN

Chris San Marchi

Sandia National Laboratories
Livermore, CA, USA

Junichiro Yamabe

Kyushu University
Fukuoka, Japan

Martina Schwarz

Materials Testing Institute of
Stuttgart, Germany

Hisao Matsunaga

Kyushu University
Fukuoka, Japan

Stefan Zickler

Materials Testing Institute of
Stuttgart, Germany

Saburo Matsuoka

Kyushu University
Fukuoka, Japan

Hideo Kobayashi

Tokyo Institute of Technology
Tokyo, Japan

ABSTRACT

Methods to qualify materials for hydrogen service are needed in the global marketplace to enable sustainable, low-carbon energy technologies, such as hydrogen fuel cell electric vehicles. Existing requirements for qualifying materials are not adequate to support growth of hydrogen technology as well as being inconsistent with the growing literature on the effects of hydrogen on fracture and fatigue. This report documents an internationally coordinated effort to develop a test method for qualifying materials for high-pressure hydrogen fuel system onboard fuel cell electric vehicles. In particular, consistency of fatigue life testing strategies is discussed. Fatigue life tests were conducted at three different institutes in high-pressure gaseous hydrogen (90 MPa) at low temperature (233K) to confirm consistency across distinct testing platforms. The testing campaign includes testing of both smooth and notched axial fatigue specimens at various combinations of pressure and temperature. Collectively these testing results provide insight to the sensitivity of fatigue life testing to important testing parameters such as pressure, temperature and the presence of stress concentrations.

INTRODUCTION

With the growth of hydrogen technologies, there is a growing need to identify strategies to select materials for hydrogen service. Careful selection of materials is important because hydrogen is known to degrade fatigue and fracture resistance of most materials. Strategies for materials selection can be of two basic forms: design

basis or performance basis. The first strategy requires definition of design requirements and measurement of materials properties. This method is the basis of pressure component codes, such as the ASME Boiler and Pressure Vessel Code, ASME Code for Pressure Piping, and many other codes that allow design by rule or design by analysis. Performance standards, on the other hand, define criteria for the performance of a material or component in a test that evaluates specific performance expectations; proof testing of pressure components is a simple type of performance test. Materials standards generally require verification that the strength and ductility of the material meets a set of minimum properties; these can also be thought of as materials performance criteria. In effect, performance-based evaluations provide pass-fail criterion for accepting a component or material for a specific application. While proof testing of pressure components and tensile testing of materials are generally accepted performance tests, these evaluations are not generally discerning or sufficient to demonstrate performance in a specific application.

Performance criteria for materials are intrinsically challenging because they are design agnostic, but ideally provide the pass-fail criteria for acceptance in actual designs. By their very nature, performance-based criteria for materials do not provide design data, rather they assess the material's suitability for the generalized service conditions. Since the materials performance evaluation does not assess a design, the performance criteria should be developed with knowledge of the materials failure mode, which implies some knowledge of the design space.

It is important to acknowledge the context of performance criteria and to not extrapolate the

performance criteria outside of their intended use. Consider, for example, the transport of gaseous hydrogen in transportable gas cylinders. Performance criteria have been established for the steels in this service application as in the ISO 11114-4 standard. The criteria in this standard are specific to the type of steels used in this application (relatively low strength Cr-Mo steels), as well as specific to the application. The performance criteria in the 11114-4 standard are not intended to be applied to other applications, as the criteria may not capture potential failure modes in other applications. For example, the ISO 11114-4 standard does not consider the fatigue performance of the steels for this application, since transportable gas cylinders generally do not see many pressurization (fatigue) cycles. Fatigue, however, can be an issue in other applications. Using transportable gas cylinders in hydrogen fuel systems creates a different usage profile, and the effects of fatigue and hydrogen should be considered. It is well known that hydrogen accelerates fatigue crack growth in Cr-Mo steels by a factor of 10 or more; therefore, additional design or performance criteria are needed to evaluate Cr-Mo steels for application in hydrogen fuel systems that may see thousands of pressurization cycles. For hydrogen-powered industrial trucks (e.g., fork lifts), the CSA HPIT1 standard, for example, imposes additional design constraints for the use of Cr-Mo transportable gas cylinders in hydrogen fuel systems to complement the performance requirements and ensure adequate performance with this different usage profile.

This study describes an international activity to develop a performance-based materials testing protocol, testing capability, and test data for the selection of materials for fuel systems onboard fuel cell electric vehicles. The testing protocol was developed to provide simple pass-fail type of criteria to assess materials for applications where many of the components are small-scale manifold type components. Moreover, the performance criteria were selected to be relevant to the application and not arbitrarily conservative.

EXPERIMENTAL PROCEDURES

Slow strain rate tensile (SSRT) tests and fatigue-life tests were performed on a SUS316L grade austenitic stainless steel. The steel was supplied as annealed bar with diameter of 25 mm. In addition, comparison of fatigue load ratio was explored with notched specimens extracted from SUS304 and SUS316L grade austenitic stainless steel plate. The compositions of the steels are provided in Table 1 and the tensile properties are summarized in Table 2.

Subsized tensile specimens in accordance with ASTM E8/E8M were machined with a diameter of 4 mm from the SUS316L bar for the SSRT testing. The specimens were tested at constant displacement rate of approximately 0.001 mm/s, which corresponds to a nominal strain rate of $5 \times 10^{-5} \text{ s}^{-1}$ for a gauge length of 20 mm.

Two variants of fatigue-life testing are considered using axially-loaded cylindrical (solid) specimens: tension-compression using a smooth specimen and tension-tension using a circumferentially notched specimen. In

both cases, fatigue testing was executed in force control at test frequency of 1 Hz with constant load amplitude (sine wave) until the specimen failed.

The smooth specimens have a minimum diameter of 6 mm over a gauge length of 18 mm. For the smooth specimen configuration, the loading was fully reversed, i.e., a load ratio, R , of -1 . The stress amplitude was 320 MPa, which is equivalent to the maximum stress.

The circumferentially notched specimen has a 60-degree, V-groove in the middle of the length and threaded ends. The net-section diameter is 4 mm at the notch root with a root radius specified as nominally 0.12 mm, while the gross section diameter is 5.7 mm. The stress concentration factor (K_t) for this geometry is about 3.9. The net-section stress is used to characterize the fatigue conditions, using the net-section diameter measured across the notch root (approximately 4 mm) for the area. The net-section stress at maximum load (S_{max}) in the notched configuration was 444 MPa with $R = 0.1$ (net-section stress amplitude of 200 MPa).

Fatigue testing was conducted at several different laboratories with different equipment. The basic environmental condition, however, was identical: gaseous hydrogen at pressure of 90 MPa and temperature of 233 K (-40°C).

In order to compare tension-compression ($R = -1$) and tension-tension ($R = 0.1$) fatigue life, additional fatigue tests were conducted using specimens extracted from the two annealed plate materials: SUS316L and SUS304. A modified circumferentially notched test specimen was utilized at a test frequency of 1 Hz in air and in 0.7 MPa hydrogen gas at room temperature. In these tests, the net-section diameter is 6.4 mm at the notch root of a 60-degree V-groove with a root radius specified as nominally 0.083 mm, while the gross section diameter is 12.8 mm. The stress concentration factor (K_t) for this geometry is about 6.6.

RESULTS

Slow strain-rate tensile tests

The materials certification for the SUS316L in this study gives a tensile strength of 551 MPa. In comparison, specifications for SUS316L (and ASTM specified grades of 316L) typically require minimum tensile strength of 480 MPa. Values of tensile strength from SSRT tests in 0.1 MPa nitrogen and 90 MPa hydrogen at temperature of 233 K are 716 and 702 MPa respectively (average of at least 3 measurements). The elongation to failure was measured post-mortem from the change in distance between reference marks on the specimen and ranged between 75 and 94%. Table 3 summarizes the SSRT measurements.

Fatigue life tests

The smooth fatigue life of SUS316L for a maximum stress of 320 MPa and full reversed loading ($R = -1$) is shown in Figure 1 along with fatigue life data from the literature. The testing in this study was conducted in gaseous hydrogen at pressure of 90 MPa and

temperature of 233 K (-40°C), while the data from literature represent tests at pressure of 115 MPa and in air at room temperature. At temperature of 233K, the fatigue life of SUS316L was equal to or slightly shorter in hydrogen gas than in nitrogen gas.

The notched fatigue life of SUS316L for a maximum net stress of 444 MPa and $R = 0.1$ is shown in Figure 2. Testing in this study includes tests from two laboratories at pressure of 90 MPa and temperature of 233 K (-40°C). Fatigue life data from the literature are also shown in Figure 2 to provide a more comprehensive view of fatigue life for this class of steels; however, the tests from the literature were conducted at pressure of 10 MPa and temperature of 223 K (-50°C).

DISCUSSION

Fatigue testing capability

In the context of hydrogen fuel cell electric vehicles, the relevant environmental conditions are pressure up to 87.5 MPa and temperature in the range 233 K (-40°C) to 358 K ($+85^{\circ}\text{C}$). Therefore, the fueling system of these vehicles will be operational across this range of conditions. The valves, fittings and manifolding of the fuel system are commonly manufactured from austenitic stainless steels. There are extensive data in the literature that show austenitic stainless steels experience a significant reduction of tensile ductility in gaseous hydrogen near the lower temperature bound for this application [1-4]. While the tensile ductility has limited usefulness in design, very little data has been reported for design relevant fracture and fatigue properties at low temperature in high pressure gaseous hydrogen. Therefore, in the absence of more relevant materials property measurements, guidance for selection of austenitic stainless steels for this application have been cautious and restrictive.

Recent advances in the availability of test data at low temperature in gaseous hydrogen suggest that the fracture and fatigue response of austenitic stainless steels does not follow the trends for tensile ductility. Fracture testing of hydrogen-precharged test samples, for example, shows only a modest effect of temperature on the fracture resistance of high-strength austenitic stainless steels and welds [5, 6]. Fatigue life testing in relatively low pressure hydrogen also show less effect on fatigue life than might be anticipated from the tensile test results [7, 8]. Fracture and fatigue testing in the combination of high pressure and low temperature, however, are only beginning to be reported [9, 10].

Execution of fatigue testing in gaseous hydrogen in the combination of high pressure (87.5 MPa) and low temperature (-40°C) is extremely challenging, although several laboratories around the world have been developing such capability. In this report, preliminary benchmark fatigue-life testing (Figure 2) shows good consistency between test laboratories for tests on the same material tested under the same environmental conditions: pressure of 90 MPa and temperature of 233 K (-40°C). Moreover, the new results are consistent with the

limited data from the literature and an important demonstration that reproducible results can be achieved for this combination of mechanical loading, pressure and temperature.

Performance-based criteria: tension

Materials selection criteria based on tensile ductility have been developed to identify materials that show minimal effect of hydrogen, particularly under conditions of rupture since tensile ductility has the most relevance to rupture compared to other failure modes. As the example of Cr-Mo steel for transportable gas cylinders shows, materials can be strongly affected by hydrogen and still be appropriate for hydrogen service (provided the service conditions and design constraints are understood). Moreover, rupture is not a likely failure mode in the normal operation of vehicle pressure systems, thus arguably not the best performance criteria for this application. It is, on the other hand, important to demonstrate that the material retains sufficient strength and ductility in the service environment and at the maximum service pressure (87.5 MPa in the case of fuel cell vehicles). Since tensile testing of materials in gaseous hydrogen can be sensitive to strain rate [11], the SSRT test in gaseous hydrogen is commonly employed to evaluate the effects of hydrogen on tensile properties. It was shown in Ref. [11] that the effects of hydrogen in tensile tests saturate for strain rate $\leq 5 \times 10^{-5} \text{ s}^{-1}$.

As mentioned in the previous section, temperature is an important consideration when evaluating the effects of hydrogen on tensile ductility, especially for austenitic stainless steels. The hydrogen testing standard CSA CHMC1 provides guidance on test temperature for SSRT testing in hydrogen for different materials classes. The minimum environmental temperature in the vehicle application of 233 K (-40°C) is consistent with the minimum tensile ductility observed for a range of austenitic stainless steels [1], and temperature within the range of $228 \pm 5 \text{ K}$ should provide consistent results.

With regard to strength metrics, it is not necessary that the strength be unchanged in hydrogen, rather the strength should remain within specified limits. Therefore, from a design and use perspective, it is important to verify that the strength of the material meets the specified minimum strength from the materials definition (e.g., the minimum strength requirements from a standard such as ASTM A479, JIS G4303, or JIS G4304 as shown in Table 2).

Additionally, the elongation and ratio of yield strength to tensile strength are commonly employed in structural design codes as simple metrics to ensure resistance to fracture. Minimum elongation values in materials specifications are based on experience with manufacturing of the alloy, not generally a particular application. In this case, the desire is a minimum performance criterion for hydrogen service in pressure applications. Therefore, a minimum value of 12% is proposed as representing a generic lower bound to ensure structural integrity in the high pressure hydrogen environment onboard the vehicle. Additionally, design codes often establish bounds on yield to tensile strength ratio to provide additional assurance of ductility and resistance to fracture. Design codes vary in the

requirements for the yield to tensile ratio, but can be as high as 0.93 [12, 13], which is the value proposed here.

In summary, the basic tensile properties of materials in the fuel system of hydrogen fuel cell electric vehicles should be evaluated by the SSRT test in gaseous hydrogen at pressure of ≥ 87.5 MPa and temperature of 228 ± 5 K. The performance requirements from this testing are:

1. yield strength and tensile strength should satisfy the specified minimum requirements from the materials specification,
2. yield to tensile ratio should be less than 0.93, and
3. elongation should exceed 12%.

In general for austenitic stainless steels, the yield strength is not changed in gaseous hydrogen [2, 3], although the tensile strength can be slightly reduced in some alloys. For the material tested here, the strength requirements exceed the specified minimums and the yield to tensile ratio is less than 0.7. In short, the tensile properties from SSRT testing of the SUS316L meet the minimum performance expectations for this alloy in high-pressure gaseous hydrogen. In general, most austenitic stainless steels are expected to satisfy these performance requirements, including high-strength austenitic stainless steels, such as Cr-Ni-Mn austenitic stainless steels and strain-hardened type 304/304L and 316/316L austenitic stainless steels.

Performance-based criteria: fatigue

For testing in fatigue, the minimum test pressure should be the maximum service pressure (≥ 87.5 MPa) as in the SSRT tests. The critical temperature of fatigue testing is less clear, mostly due to lack of data. In the case of the SSRT test, an environmental temperature of 228 ± 5 K was defined as the most discerning temperature. Tensile data suggest that the hydrogen effects will be most apparent at low temperature; however, the hydrogen effects on tensile properties manifest primarily at very high strains, which are generally absent from fatigue testing. Emerging data for austenitic stainless steels suggest that fatigue life is improved at low temperature [10]. This trends can be attributed to the tendency for the yield and tensile strength to increase as the temperature is lowered in austenitic stainless steels. In short, the limiting fatigue performance of austenitic stainless steels in hydrogen may not be at low temperature. More data is necessary to confirm this hypothesis and may depend on the class of material, thus, until more comprehensive data is available, fatigue testing is recommended at both room temperature and 228 ± 5 K.

To establish fatigue performance requirements in hydrogen, it is important to consider both the cycle life requirements for the application and mechanical loading conditions. The primary fatigue stress onboard the vehicle originates from the pressurization of the fuel system; in other words, the number of times the vehicle is refueled. Even if refueled every day for 10 years, the number of pressure/stress cycles on the fuel system would be less than 5,000. While different standards specify different lifetime requirements for fuel cell vehicles, in all cases, the number of fatigue cycles in this application is

relatively low. The stress in the materials will also be modest since design stresses in high-pressure systems are usually low. Of course, the specifics of the stresses depend on the employed design methodology, as well as the details of the design, both of which are beyond the scope of performance-based criteria. However, considering the maximum allowable stresses in applicable design codes (such as the ASME Code for Pressure Piping) as a general guide, stresses should be less than about 1/3 of the specified minimum tensile strength. Using these general constraints on the design space, a conservative, materials-based fatigue life performance requirement can be proposed as $>100,000$ cycles for a maximum applied stress of 1/3 the measured tensile strength.

In the case of smooth specimens, the fatigue limit of annealed austenitic stainless steels is not affected by hydrogen, although finite fatigue life is generally degraded as shown in the experimental data of Figure 1 [14]. A stress amplitude of 1/3 the measured tensile strength corresponds with a lower bound of the fatigue limit for smooth specimens at R of -1 , and the number of cycles at the knee point (the abrupt change in slope of the fatigue curve) appears around 200,000 cycles. Therefore, a performance metric of $>200,000$ cycles for smooth specimens tested with stress amplitude of 1/3 the measured tensile strength evaluates whether the fatigue limit of annealed austenitic stainless steels is degraded or not in high-pressure gaseous hydrogen.

These fatigue performance requirements are conservative with respect to number of cycles by a factor of about 10 or more in practice (depending on the specific life requirement). Additionally, the requirement of testing at 1/3 the measured tensile strength is also conservative, since the lower bound of the fatigue limit is characterized by the specified minimum tensile strength. In other words, the net-section stress for testing will always be greater than the design stress, if the design stress is characterized by the lower bound fatigue limit or 1/3 of the specified minimum tensile strength.

The measurement of fatigue life at a single stress level provides a simple, performance-based method to assess materials for this application. While this evaluation enables a consistent and relevant method to assess the fatigue performance of materials when conducted in the service environment, it is not intended to validate the design or to provide design data. Since the materials performance evaluation is agnostic to design specifics, the fatigue methodology can be flexible and does not necessarily need to be consistent with state-of-the-art, strain-based fatigue methodologies. Indeed, the proposed performance criterion is a stress-based criterion. In addition, the specimen configuration does not need to be limited to classic fully-reversed loading. Indeed, in the pressure application, the stresses are generally tension-tension. As such, two test configurations are proposed:

1. tension-compression loading of a smooth axially-loaded specimen, R of -1 , or
2. tension-tension loading of a circumferentially notched axially-loaded specimen, R of 0.1

These two specimens were described in the experimental procedures section, each having advantages and disadvantages. The smooth tension-compression configuration represents the fundamental fatigue test

configuration and can ordinarily be used for strength design for various components by using the fatigue notch factor and mean-stress correction. The tension-compression loading configuration, however, is challenging to execute in high-pressure systems. In contrast, the notched tension-tension configuration is arguably less conventional, but the tension-tension loading is less challenging to execute in high-pressure systems. Additionally, the notched tension-tension configuration can simulate the tension-tension loading in pressure systems as well as simulating the effect of stress concentrations that invariably exist in real applications. The relationship between the smooth tension-compression configuration and the notched tension-tension configuration will be discussed in the following section.

In summary, two options for establishing fatigue life performance in gaseous hydrogen are identified:

1. >200,000 cycles for smooth tension-compression fatigue life tests with R of -1 , or
2. >100,000 cycles for notched tension-tension fatigue life tests with $R = 0.1$.

In both cases, the maximum load must correspond to a net-section stress of $1/3$ the measured tensile strength. From a materials selection perspective where S_{max} is the governing metric, the smooth tension-compression configuration evaluates whether the fatigue limit is substantially changed in gaseous hydrogen. In contrast, the notched tension-tension configuration ($R = 0.1$) requires a conservative fatigue life (>100,000 cycles) in gaseous hydrogen at S_{max} consistent with the fatigue limit in a smooth specimen and zero mean stress (F_r). Therefore, while it may not guarantee infinite life, the notched configuration demonstrates that the material can sustain sufficient fatigue life for the vehicle application in the presence of a stress concentration at net-section stress consistent with the fatigue limit.

Literature data can be easily placed into the context of the proposed performance metrics by normalizing the maximum stress by the tensile strength, as shown in Figure 1 for the smooth tension-compression configuration. Normalized data for the notched tension-tension configuration are shown in Figure 2a – in this figure, the literature data is normalized by the tensile strength at the test temperature (since the tensile strength at room temperature was not reported), which adds additional conservatism since the tensile strength is certainly greater at the test temperature than at room temperature. This representation of the data clearly show that austenitic stainless steels appear to satisfy these performance criteria. The normalization of S_{max} by the tensile strength also eliminates some of the apparent scatter in the fatigue curves; for example, the data from Ref. [9] represent the same alloy in the annealed and strain-hardened condition, when the strength difference is considered the curves for the two conditions collapse (open squares and diamonds) to a single curve. Similar convergence in Figure 2a is also apparent for some of the materials from Ref. [8].

Comparison of notched to smooth fatigue

The fatigue life tests of the notched and smooth configurations can be compared in the fatigue limit by

considering the effects of the mean stress (S_M) and the fatigue notch factor (K_f). There are several ways to estimate the effect of the mean stress on fatigue life curves. A common (and generally conservative) construction for mean stress corrections is the Goodman relationship [15]. For most metals, the Smith-Watson-Topper (SWT) method provides a better correction [15], where stress amplitude for zero mean stress (S_{ar}) is determined from the maximum stress (S_{max}) and the stress amplitude (S_a) as

$$S_{ar} = \sqrt{S_{max}S_a} = S_{max} \sqrt{\frac{1-R}{2}} \quad (1)$$

Empirically, the fatigue limit of the notched configuration (F_{Nr}) is related to the fatigue limit in the smooth configuration (F) by [16]

$$F_{Nr} = F_r / K_f \quad (2)$$

where K_f is the fatigue notch factor (generally less than the elastic stress concentration factor K_t) and the subscript r denotes the zero mean stress condition. Recognizing that the fatigue limit is just the stress amplitude, and combining these two equations for the notched configuration gives

$$S_{max,FL} = \frac{F_r}{K_f} \sqrt{\frac{2}{1-R}} \quad (3)$$

where $S_{max,FL}$ is the maximum stress in the fatigue limit.

For $R = -1$ and $K_f = 1$, equation 3 reduces to $S_{max,FL} = F_r$ as expected for fully reversed loading in a smooth specimen: the stress amplitude in the fatigue limit (F_r) is the maximum fatigue stress ($S_{max,FL}$). In the case of $R = 0.1$, $S_{max,FL}$ is less than F_r when $K_f > \sim 1.5$, which implies that the notched tension-tension configuration is conservative with respect to the smooth tension-compression configuration, when using $S_{max,FL}$ as a surrogate for F_r . Moreover, due to the nature of fatigue life curves, the notched tension-tension configuration with $K_f > 1.5$ and $R \leq 0.1$ will always result in a fatigue curve expressed as S_{max} that is conservative relative to smooth tension-compression ($R = -1$ and $K_f = 1$).

The relationship between the fatigue life curves in terms of S_{max} for both the smooth tension-compression configuration ($R = -1$ and $K_f = 1$) and the notched tension-tension configuration ($R = 0.1$ and $K_f > 1.5$) is shown schematically in Figure 5a. A schematic of the applied stress cycle is also shown in Figure 5b for the same maximum stress, emphasizing the difference in the load/stress cycle for the two configurations. While comparison of the two fatigue test configurations may not be directly obvious when plotting fatigue data in terms of stress amplitude, plotting in terms of S_{max} as in Figure 5a demonstrates the relationship between the data evaluated by these two configurations. As mentioned previously, for S_{max} near F_r , specimens tested in the notched tension-tension configuration may display finite life if $\sqrt{2/(1-R)}/K_f$ is sufficiently less than 1.

Additionally, the fatigue life in the notched condition should decrease for larger K_f .

The relationship between the fatigue life curves for the notched tension-compression configuration and the notched tension-tension configuration was experimentally investigated with SUS304 and SUS316L in air and in hydrogen gas at pressure of 0.7 MPa at room temperature. Notched fatigue properties of SUS316L at $R = -1$ and $R = 0.1$ are shown in Figure 3, whereas those of SUS304 at $R = -1$ and $R = 0.1$ are shown in Figure 4. As apparent in Figure 4, hydrogen can reduce the fatigue life in the low-cycle regime, while hydrogen does not affect fatigue life in the high-cycle regime. Furthermore, Figures 3b and 4b reveal that the mean-stress effect (S_{ar}) on the fatigue limit of SUS316L and SUS304 was successfully corrected by equation (1) based on the SWT method. The fatigue limits of the notched configuration under the zero mean stress condition (F_{Nr}) were 180 MPa for SUS304 and 80 MPa for SUS316L, respectively. According to Figure 1, the fatigue limit of the smooth configuration under the zero mean stress condition (F_r) for annealed austenitic stainless steels is $0.37S_u$ (at a fracture probability of 50%): $F_r = 235$ MPa (SUS304) and 195 MPa (SUS316L). Therefore, the fatigue notch factor (K_f) is estimated to be 1.3 for SUS304 and 2.4 for SUS316L. Additionally, based on the literature, the K_f value of Cr-Mo steel ($S_u = 861$ MPa) is 3.3 [17] and the K_f values of the present steels were approximately 1.5 or higher.

SUMMARY

- Fatigue life testing in gaseous hydrogen under the combination of high pressure (90 MPa) and low temperature (233 K) was demonstrated and consistent results were produced at multiple laboratories on specimens from the same material.
- Pass-fail type performance-based criteria were established for high-pressure hydrogen service in the vehicle application. These criteria include demonstrating that the material maintains strength properties and minimal ductility in gaseous hydrogen as well as achieves a minimum fatigue life benchmark. The benchmark ensures that the fatigue life of the material will exceed a generic description of the design space for the application without specific definition of the design.
- Either of two fatigue test configurations are proposed for assessment of fatigue performance in gaseous hydrogen. The smooth configuration evaluates the fatigue limit in presence of hydrogen ($R = -1$). The notched configuration ($R = 0.1$), on the other hand, verifies a conservative life for the vehicle application in the presence of a stress concentration at net-section stresses consistent with the fatigue limit (F_r).

ACKNOWLEDGMENTS

Sandia National Laboratories is a multi-program laboratory managed and operated by National Technology and Engineering Solutions of Sandia, LLC., a

wholly owned subsidiary of Honeywell International, Inc., for the U.S. Department of Energy's National Nuclear Security Administration under contract DE-NA-0003525. This work was also partially supported by the New Energy and Industrial Technology Development Organization (NEDO), Hydrogen Utilization Technology (2013 to 2018). The Materials Testing Institute of Stuttgart is provided with funding for the project from the Federal Ministry of Transport and Digital Infrastructure (BMVI) through the "National Innovation Programme for Hydrogen and Fuel Cell Technology." The programme is coordinated by the NOW GmbH National Organisation Hydrogen and Fuel Cell Technology.

REFERENCES

1. S. Fukuyama, D. Sun, L. Zhang, M. Wen and K. Yokogawa, Effect of Temperature on Hydrogen Environment Embrittlement of Type 316 Series Austenitic Stainless Steels at Low Temperature, *J Japn Inst Metals* 67 (2003) 456-459.
2. T. Michler and J. Naumann, Hydrogen environment embrittlement of austenitic stainless steels at low temperatures, *Int J Hydrogen Energy* 33 (2008) 2111-2122.
3. T. Michler, A.A. Yukhimchuk and J. Naumann, Hydrogen environment embrittlement testing at low temperatures and high pressures, *Corros Sci* 60 (2008) 3519-3526.
4. L. Zhang, M. Wen, M. Imade, S. Fukuyama and K. Yokogawa, Effect of nickel equivalent on hydrogen gas embrittlement of austenitic stainless steels based on type 316 at low temperatures, *Acta Mater* 56 (2008) 3414-3421.
5. H.F. Jackson, C. San Marchi, D.K. Balch and B.P. Somerday, Effect of low temperature on hydrogen-assisted crack propagation in 304L/308L austenitic stainless steel fusion welds, *Corros Sci* 77 (2013) 210-221.
6. H.F. Jackson, C. San Marchi, D.K. Balch, B.P. Somerday and J. Michael, Effects of low temperature on hydrogen-assisted crack growth in forged 304L austenitic stainless steel, *Metall Mater Trans* 47A (2016) 4334-4350.
7. T. Michler, J. Naumann and E. Sattler, Influence of high pressure gaseous hydrogen on S-N fatigue in two austenitic stainless steels, *Intern J Fatigue* 51 (2013) 1-7.
8. T. Michler, J. Naumann, J. Wiebesiek and E. Sattler, Influence of frequency and wave form on S-N fatigue of commercial austenitic stainless steels with different nickel contents in inert gas and in high pressure gaseous hydrogen, *Intern J Fatigue* 96 (2017) 67-77.
9. C. San Marchi, P. Gibbs, J. Foulk and K. Nibur, Fatigue life of austenitic stainless steels in hydrogen environments, in: 43rd MPA Seminar (Stuttgart, Germany, 2017),
10. T. Iijima, H. Enoki, J. Yamabe and B. An, Effect of high pressure gaseous hydrogen on fatigue properties of SUS304 and SUS316 austenitic stainless steel (PVP2018-84267), in: Proceedings of the ASME 2018 Pressure Vessels and Piping

- Division Conference (Prague, Czech Republic, 2018), 15-20 July 2018,
11. H. Kobayashi, T. Yamada, H. Kobayashi and S. Matsuoka, Criteria for selecting materials to be used for hydrogen refueling station equipment (PVP2016-64033), in: Proceedings of the ASME 2016 Pressure Vessels and Piping Division Conference (Vancouver, British Columbia, Canada, 2016), ASME, 17-21 July 2016,
 12. A.C. Bannister, J. Ruiz Ocejo and F. Gutierrez-Solana, Implications of the yield stress/tensile stress ratio to the SINTAP failure assessment diagrams for homogeneous materials, Eng Fract Mech 67 (2000) 547-562.
 13. H.A. Ernst, R.E. Bravo, J.A. Villasante and A. Izquierdo, Effect of the yield to tensile ratio on structural integrity of linepipes subjected to internal pressure, Journal of Offshore Mechanics and Arctic Engineering 133 (2011) 031401.
 14. M. Nakamura, S. Okazaki, H. Matsunaga and S. Matsuoka. Fatigue life properties of austenitic stainless steel welds in high-pressure hydrogen gas in: JSME M&M2017 Conference (Hokkaido, Japan, 2017).
 15. N.E. Dowling, C.A. Calhoun and A. Arcari, Mean stress effects in stress-life fatigue and the Walker equation, Fatigue Fract Eng Mater Struct 32 (2009) 163-179.
 16. J. Schijve, Fatigue of Structures and Materials, Kluwer Academic Publishers, New York, 2004.
 17. J. Yamabe, H. Matsunaga, Y. Furuya, S. Hamada, H. Itoga, M. Yoshikawa, E. Takeuchi and S. Matsuoka, Qualification of chromium-molybdenum steel based on the safety factor multiplier method in CHMC1-2014, Int J Hydrogen Energy 40 (2015) 719-728.

Table 1. Compositions (wt%) of the austenitic stainless steels.

Alloy	Fe	Cr	Ni	Mn	Mo	Si	C	S	P
SUS316L bar ¹	Bal	17.13	12.19	1.41	2.05	0.49	0.019	0.024	0.029
SUS316L plate ²	Bal	17.45	12.09	0.84	2.05	0.50	0.018	<0.001	0.021
SUS304 plate ²	Bal	18.16	8.09	0.84	-	0.42	0.06	0.002	0.030

1) This steel was used for the interlaboratory testing.

2) These steels were used for comparison of notched to smooth fatigue.

Table 2. Tensile properties of austenitic stainless steels.

Alloy	Source/Standard	S_y (MPa)	S_u (MPa)	E/t (%)	RA (%)
SUS316L bar ¹	Mill certification	245	551	60	78
SUS316L plate ²	Mill certification	229	528	76	-
SUS304 plate ²	Mill certification	274	628	63	-
304L/316L annealed bar	ASTM A479	170 minimum	485 minimum	30 minimum	40 minimum
SUS304L/316L annealed bar or plate	JIS G 4303 (bar) JIS G 4304 (plate)	175 minimum	480 minimum	40 minimum	60 minimum ³
SUS304/316 annealed bar or plate	JIS G 4303 (bar) JIS G 4304 (plate)	205 minimum	520 minimum	40 minimum	60 minimum ³

- 1) This steel was used for the interlaboratory testing.
- 2) These steels were used for comparison of notched to smooth fatigue.
- 3) RA is specified only in JIS G 4303 (i.e., for bar).

Table 3. SSRT test results measured at 233K (-40°C) for SUS316L austenitic stainless steel bar.

Environment	Tensile strength (MPa)	Elongation (%)	RA (%)
0.1 MPa N ₂	716	85	84
90 MPa H ₂	702	83	67

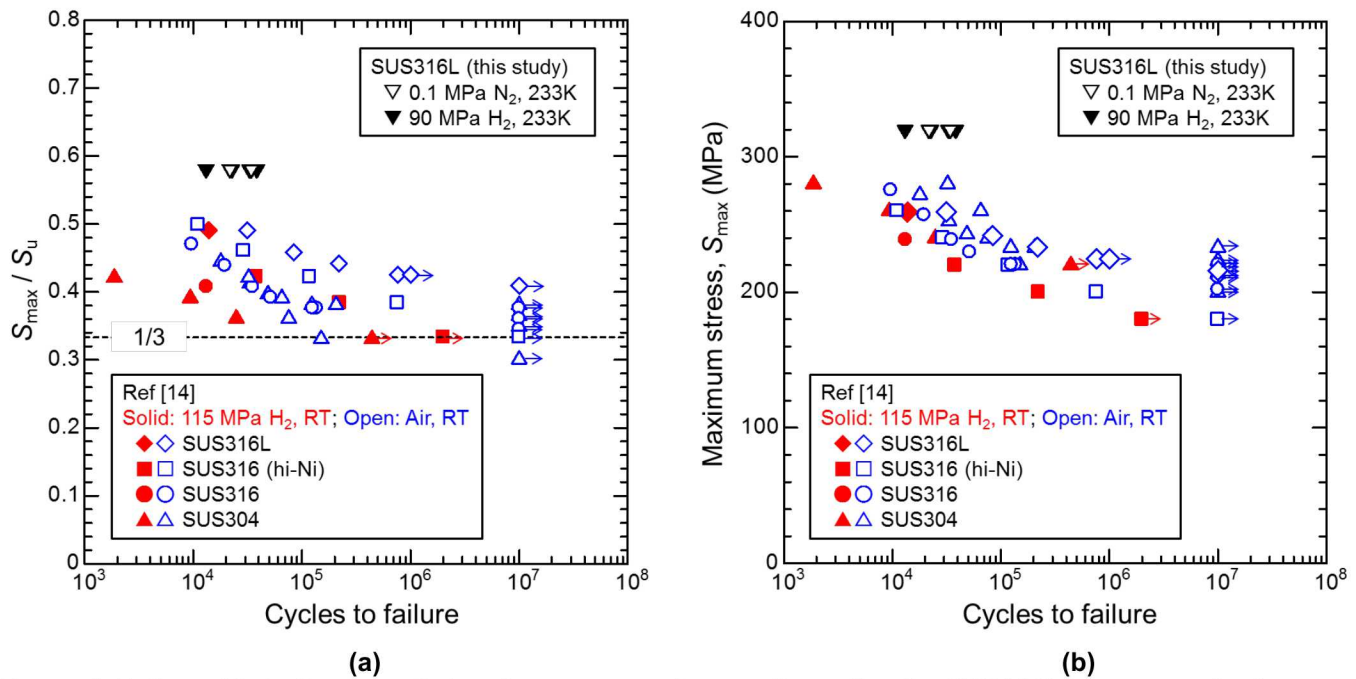


Figure 1. Fatigue life in the smooth tension-compression configuration for SUS316L in gaseous hydrogen at pressure of 90 MPa and temperature of 233 K compared with data from the literature (115 MPa / RT). (a) Normalized S-N curves. (b) S-N curves.

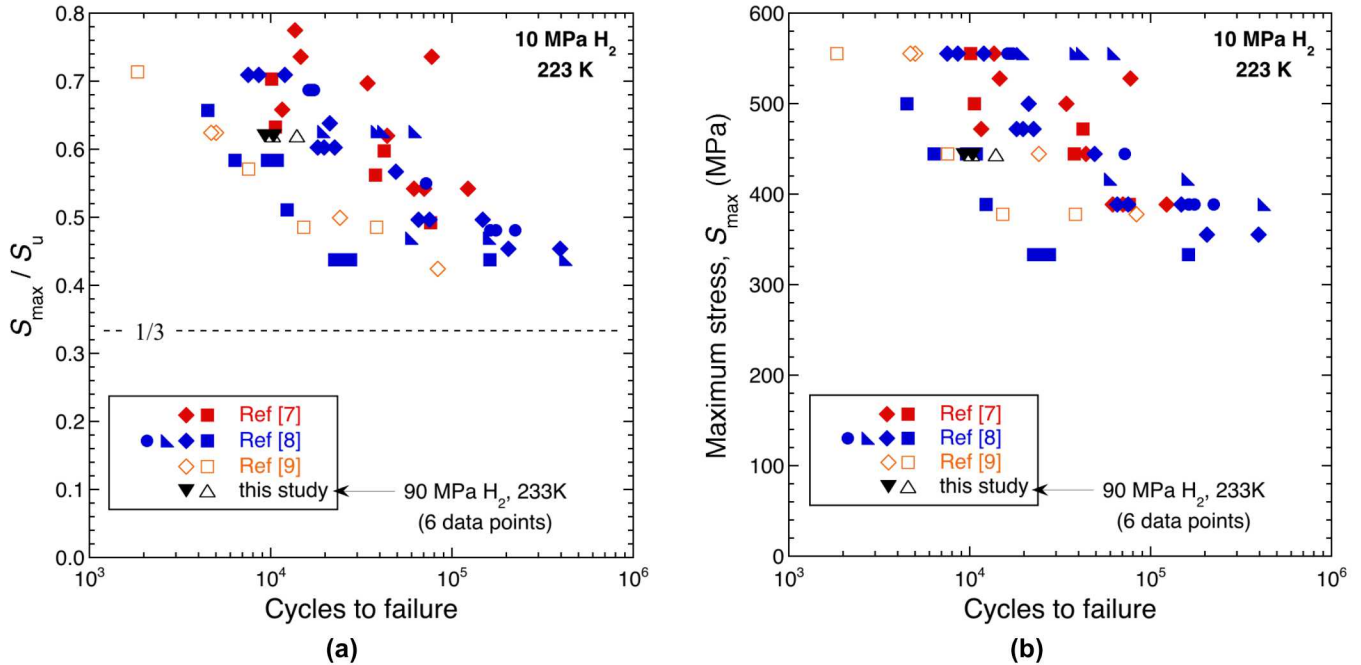


Figure 2. Fatigue life in the notched tension-tension configuration for SUS316L in gaseous hydrogen at pressure of 90 MPa and temperature of 233 K compared with data from the literature (10 MPa / 223K). (a) Normalized S-N curves. (b) S-N curves.

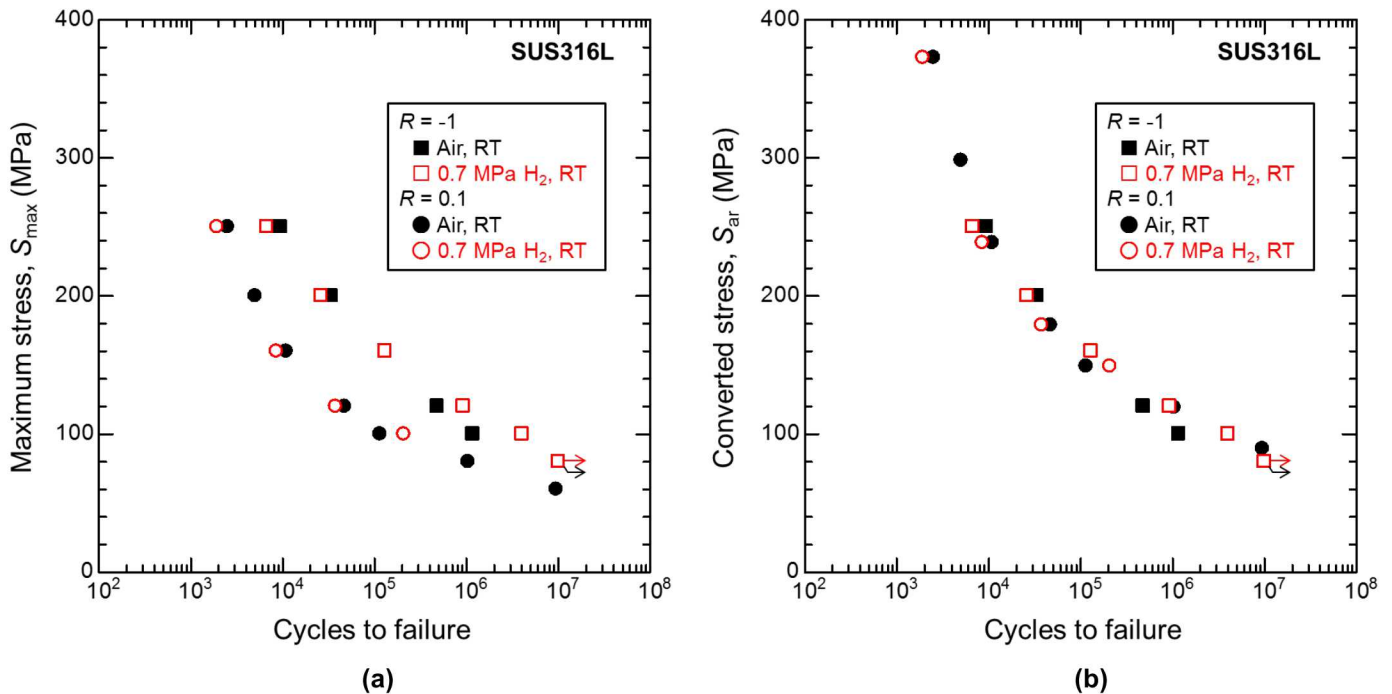


Figure 3. Fatigue life in the notched tension-compression and notched tension-tension configurations for SUS316L in gaseous hydrogen at pressure of 0.7 MPa and in air at room temperature. (a) Fatigue life based on maximum stress. (b) Fatigue life based on converted stress.

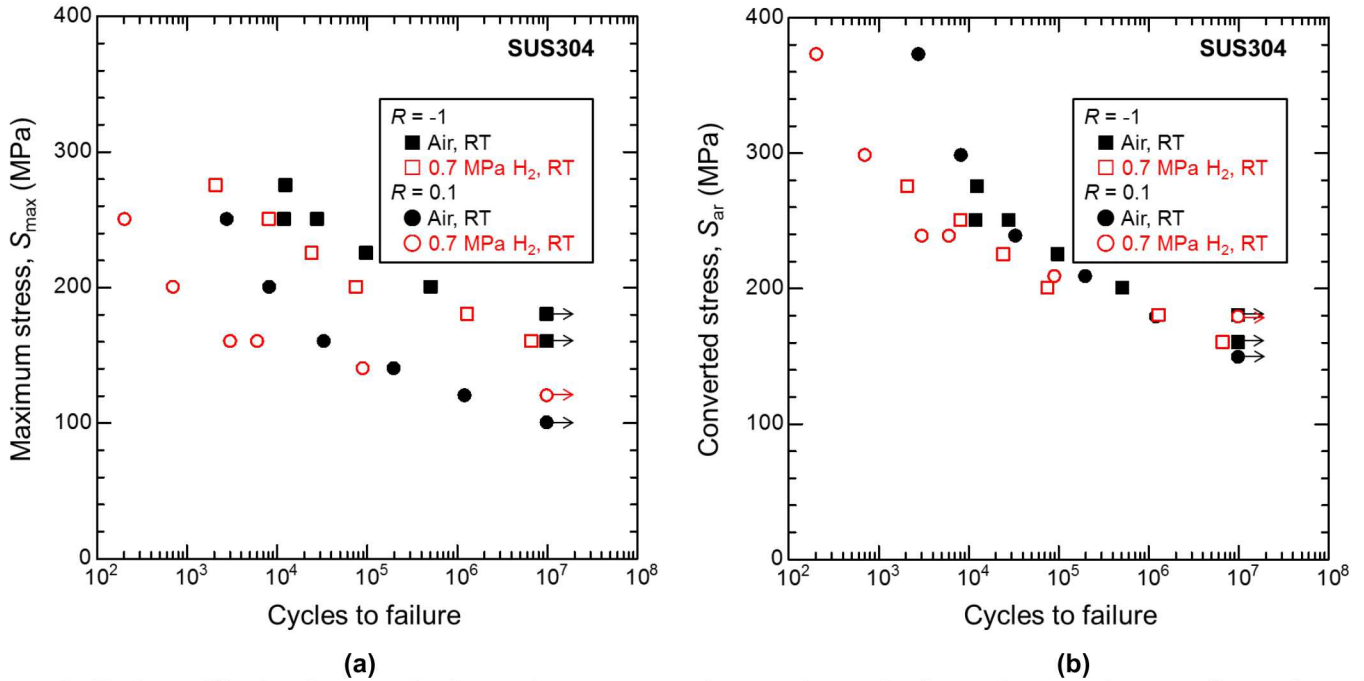


Figure 4. Fatigue life in the notched tension-compression and notched tension-tension configurations for SUS304 in gaseous hydrogen at pressure of 0.7 MPa and in air at room temperature. (a) Fatigue life based on maximum stress. (b) Fatigue life based on converted stress.

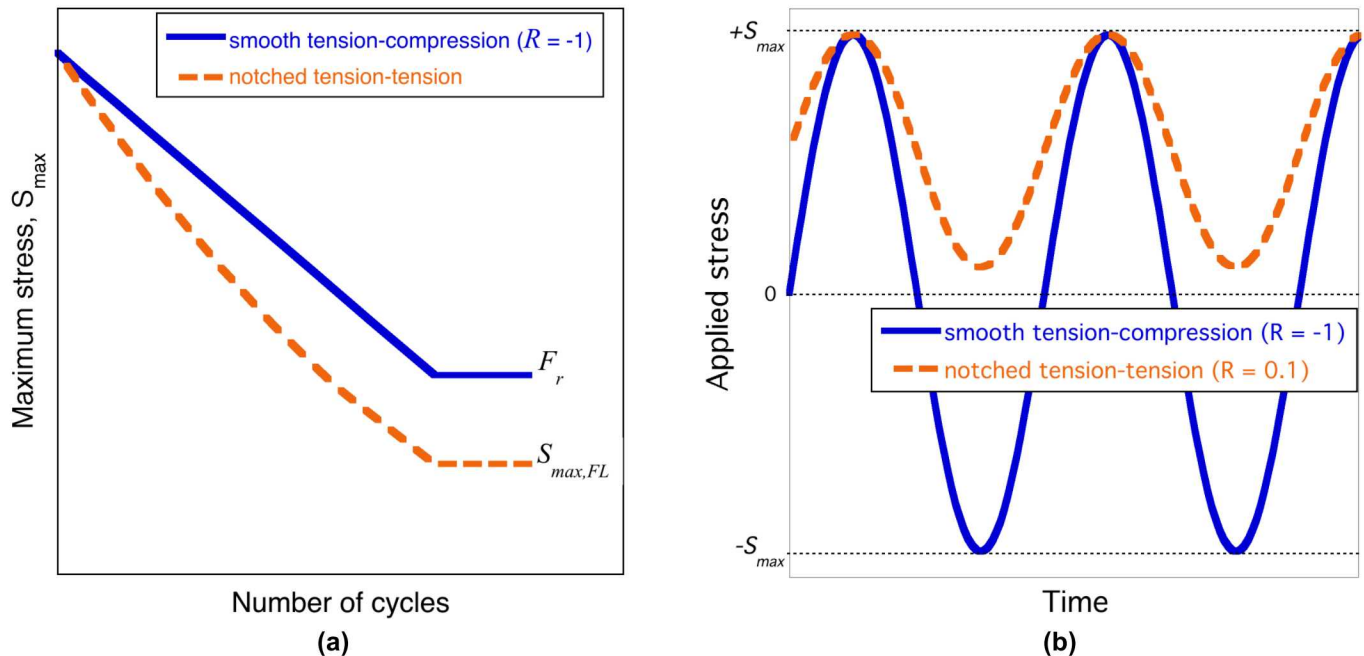


Figure 5. (a) Schematic of fatigue life curves in terms of the maximum stress for both the smooth tension-compression configuration and the notched tension-tension configuration. (b) Stress cycle for both test configurations with the same net section stress at the maximum applied load.